

Electronic structure and magnetic states in $\text{La}_{1-x}\text{Sr}_x\text{CoO}_3$ studied by photoemission and x-ray-absorption spectroscopy

T. Saitoh,* T. Mizokawa, and A. Fujimori

Department of Physics, University of Tokyo, Bunkyo-ku, Tokyo 113, Japan

M. Abbate

Laboratorio Nacional de Luz Sincrotron, Caixa Postal 6192, Campinas, 13081-970, Brazil

Y. Takeda

Department of Chemistry, Faculty of Engineering, Mie University, Tsu 514, Japan

M. Takano

Institute for Chemical Research, Kyoto University, Uji, Kyoto 611, Japan

(Received 12 February 1997)

We have studied the effects of hole doping on the electronic structure of $\text{La}_{1-x}\text{Sr}_x\text{CoO}_3$ by photoemission and x-ray-absorption spectroscopy. The Co $2p$ core-level and the valence-band spectra show charge-transfer satellites, which have been more obviously observed in $3p$ - $3d$ resonant-photoemission spectra. By Sr substitution for La in LaCoO_3 , the valence-band spectra do not show rigid-band behavior but change systematically and reflect the semiconductor-to-metal transition which occurs with hole doping. Only small changes with x have been observed in the resonant-photoemission spectra. Combined with configuration-interaction cluster-model calculations, this observation suggests that the intermediate-spin state is realized in the ferromagnetic phase. [S0163-1829(97)05828-1]

I. INTRODUCTION

Numerous studies on perovskite-type manganese oxides $\text{La}_{1-x}\text{A}_x\text{MnO}_3$ ($A = \text{Ca}, \text{Sr}, \text{or Ba}$) have been made because of their huge negative magnetoresistance (MR) called colossal magnetoresistance.¹ In these compounds, metallic conductivity realized by a proper amount of hole doping is accompanied by ferromagnetism. This has been in principle understood as due to the double exchange mechanism.²

There is another system which shows fairly large MR: Co perovskites $\text{La}_{1-x}\text{A}_x\text{CoO}_3$ ($A = \text{Ca}, \text{Sr}, \text{or Ba}$). MR in bulk³ and thin films⁴ has been observed only recently. The parent compound LaCoO_3 is a nonmagnetic (low-spin) semiconductor at low temperatures but it undergoes a gradual transition from the nonmagnetic ground state to a paramagnetic state above ~ 90 K and then to a metal above ~ 500 K. It has been controversial whether the 90-K transition is a low-spin-to-high-spin one or not. Recently, an interpretation that the transition is a low-spin-to-intermediate-spin one has been proposed by an electronic structure calculation study⁵ and a detailed spectroscopic study.⁶ Previous work on LaCoO_3 is reviewed in Ref. 6.

By replacing La by Sr, one can introduce holes into LaCoO_3 . Then the system changes from the nonmagnetic semiconductor to a ferromagnetic metal up to the Sr end,⁷⁻⁹ implying that $\text{La}_{1-x}\text{Sr}_x\text{CoO}_3$ is an example of double exchange systems like $\text{La}_{1-x}\text{Sr}_x\text{MnO}_3$. In fact, a fairly large negative MR has been observed by Yamaguchi *et al.*³ However, the saturation moment in the ferromagnetic phase ($0.3 > x$) is only about half of the full moment of the high-spin Co ion^{7,9} while $\text{La}_{1-x}\text{Sr}_x\text{MnO}_3$ shows the full moment

for $0.2 \leq x \leq 0.4$.¹⁰ Itoh *et al.* have shown that lightly doped samples ($0.0 < x \leq 0.18$) are in the spin-glass state and that heavily doped ones ($0.18 \leq x \leq 0.6$) are in the (ferromagnetic) cluster-glass state.¹¹ Chainani, Mathew, and Sarma¹² have observed a semiconductor-to-metal transition with Sr doping in ultraviolet photoemission (UPS) and bremsstrahlung isochromat spectra, but the data did not show a large change in spite of the nonmagnetic-to-ferromagnetic transition. Recently, Potze, Sawatzky, and Abbate¹³ have studied x-ray absorption (XAS) spectra of SrCoO_3 , and concluded that SrCoO_3 has the intermediate-spin ($t_{2g}^4 e_g^1$, $S = 3/2$) ground state. They have also pointed out the possibility of an intermediate-spin state in lightly doped LaCoO_3 . However, there have been few studies so far from the viewpoint of the double exchange mechanism,^{3,4,14} especially by photoemission spectroscopy. In this paper, we present the results of x-ray photoemission (XPS), UPS, resonant photoemission, and XAS studies on $\text{La}_{1-x}\text{Sr}_x\text{CoO}_3$ and discuss hole-doping effects on the electronic structure. We also discuss the smaller MR ratio of the present system than the Mn oxides.

II. EXPERIMENT

Polycrystalline samples of $\text{La}_{1-x}\text{Sr}_x\text{CoO}_3$ were prepared by a solid-state reaction. Sintered mixtures of appropriate molar quantities of La_2O_3 , SrCO_3 , and Co_3O_4 were pressed into pellets. Subsequent processing for each sample is as follows: for LaCoO_3 and $\text{La}_{0.8}\text{Sr}_{0.2}\text{CoO}_3$, pellets were fired in O_2 atmosphere at 900°C for 48 h, at 1200°C for 24 h, and at 1300°C for 24 h, and then slowly cooled to room temperature. For $\text{La}_{0.6}\text{Sr}_{0.4}\text{CoO}_3$ and $\text{La}_{0.4}\text{Sr}_{0.6}\text{CoO}_3$, the

pellets were further annealed under O_2 pressure of 300 atm at 350 °C for 82 h after the above process. For $La_{0.2}Sr_{0.8}CoO_3$ and $SrCoO_3$, pellets were fired at 1300 °C in a N_2 gas flow, quenched into liquid N_2 , and annealed under the O_2 pressure of 200 atm at 350 °C. Stoichiometric $SrCoO_3$ was obtained by using a high pressure apparatus in which the oxygen-deficient composition sealed in a gold capsule with an oxygen generator $KClO_4$ was treated at 6 GPa at 600 °C.

XPS and UPS measurements were performed using a spectrometer equipped with a $Mg K\alpha$ source, a He discharge lamp and a Physical Electronics (PHI) double-pass cylindrical-mirror analyzer. UPS spectra including $3p$ - $3d$ resonant-photoemission spectra were measured at beamline BL-2 of Synchrotron Radiation Laboratory (SRL), Institute for Solid State Physics, University of Tokyo. $O 1s$ XAS measurements were performed at BESSY in Berlin. All the measurements were carried out at liquid-nitrogen temperatures (~ 80 K). The base pressures in the spectrometer were in the low 10^{-10} Torr range. Binding energies in photoemission spectra have been calibrated using the Fermi edge of Au evaporated onto samples. For the XPS spectra, the $Au 4f_{7/2}$ (84.0 eV) core level was also used. Photon energies of XAS spectra have been calibrated using the $O 1s$ absorption peak of TiO_2 at 530.7 eV. The energy resolution of the XPS, He I UPS, and He II UPS measurements using the PHI system was ~ 0.9 , ~ 0.25 , and ~ 0.35 eV full width at half maximum (FWHM), respectively. The energy resolution of the measurements at SRL was 0.3–0.4 eV FWHM for photon energies from 40 to 80 eV. In the XAS measurements, the resolution was ~ 0.2 eV.

Clean surfaces have been obtained by scraping the samples *in situ* with a diamond file at ~ 80 K. In the case of XPS, the scraping was made until the $O 1s$ core-level spectrum became a single peak and did not change with further scraping. A shoulder or a tail on the higher binding-energy side of the $O 1s$ peak is usually associated with contamination or degradation of the surface. Figure 1 shows that such a contamination or degradation is small particularly for small x 's. In the case of UPS, scraping was repeated until a bump around 9–10 eV disappeared and the whole spectrum did not change with further scraping. We paid attention to the intensity of this bump and of a structure around 6 eV, which increase in time due to aging of the surface. We estimated how long a fresh surface lasted by observing the change in the $O 1s$ spectrum and the valence-band spectrum for XPS and UPS, respectively, and scraped the sample before aging. The lifetime was typically 1–2 h for XPS and ~ 30 min to 1 h for UPS.

III. RESULTS

In Fig. 2, $Co 2p$ core-level XPS spectra for various Sr concentrations are shown. All the spectra have $2p_{3/2}$ and $2p_{1/2}$ spin-orbit doublet peaks located at ~ 780 and ~ 796 eV, respectively. The broad peaks located around 790 and 806 eV are charge-transfer satellites of the $2p_{3/2}$ and $2p_{1/2}$ peaks, respectively, in good agreement with previous reports.^{12,15} Although all the compositions display the satellite structure, the intensity slightly decreases with Sr concentration. We have also measured $La 3d$ core-level XPS spec-

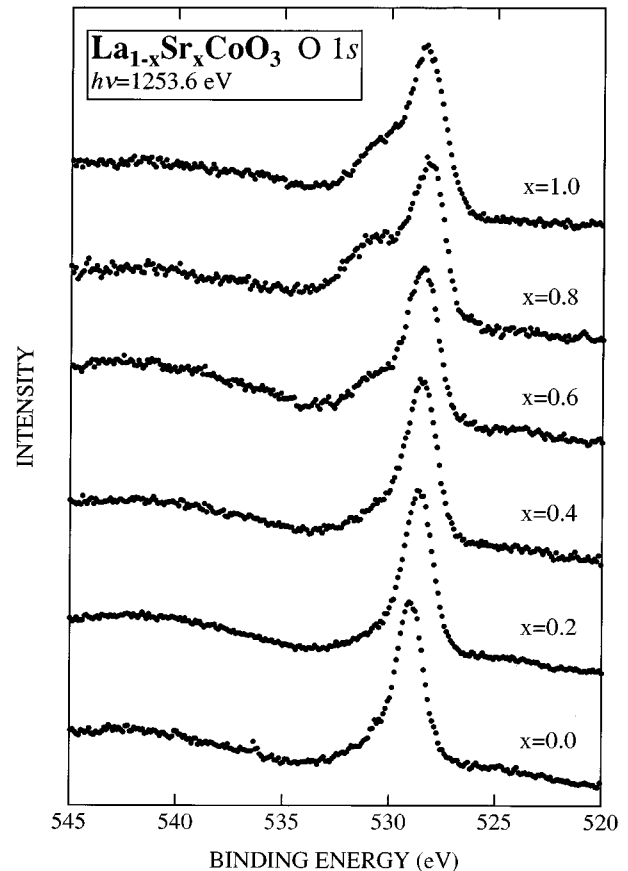


FIG. 1. $O 1s$ core-level XPS spectra of $La_{1-x}Sr_xCoO_3$. The broad peak around 540 eV is due to $Co L_{3M_{23}V}$ and $La M_{45}N_{45}V$ Auger emissions.

tra (not shown). We shall discuss below energy shifts of the core levels ($O 1s$, $Co 2p$, and $La 3d$) and the valence band as a function of Sr concentration.

Figure 3 shows He II spectra of $La_{1-x}Sr_xCoO_3$. One can see four structures A, B, C, and D as indicated in the figure. The most obvious hole-doping effect is the decrease of the intensity at structure A. One can also notice that structures in the valence band becomes less sharp. In order to see the changes with hole doping in more detail, we have subtracted the background due to secondary electrons from each of the spectra and normalized them to the integrated intensity. The resulting spectra are shown in the upper panel of Fig. 4. Now it is very clear that structure A becomes weaker with x and a weak tail develops on the lower binding-energy side and crosses E_F . Hence, with the collapse of structure A, the valence band is shifted towards E_F and thus the spectral intensity at E_F monotonously increases to the extent similar to other metallic $3d$ transition-metal oxides. The intensity is much higher than that of $La_{1-x}Sr_xMnO_3$.^{16,17} Those experimental findings are in agreement with the recent XPS study of $La_{1-x}Ca_xCoO_3$.¹⁸

It should be noted that the spectral line shape from structure C to edge E is not affected significantly by Sr doping, as shown in the lower panel of Fig. 4. In the lower panel, the spectra from $x=0.2$ to $x=0.6$ have been shifted so that edge E is aligned. With these shifts, the region between E and C in all the spectra are found to overlap well, meaning that

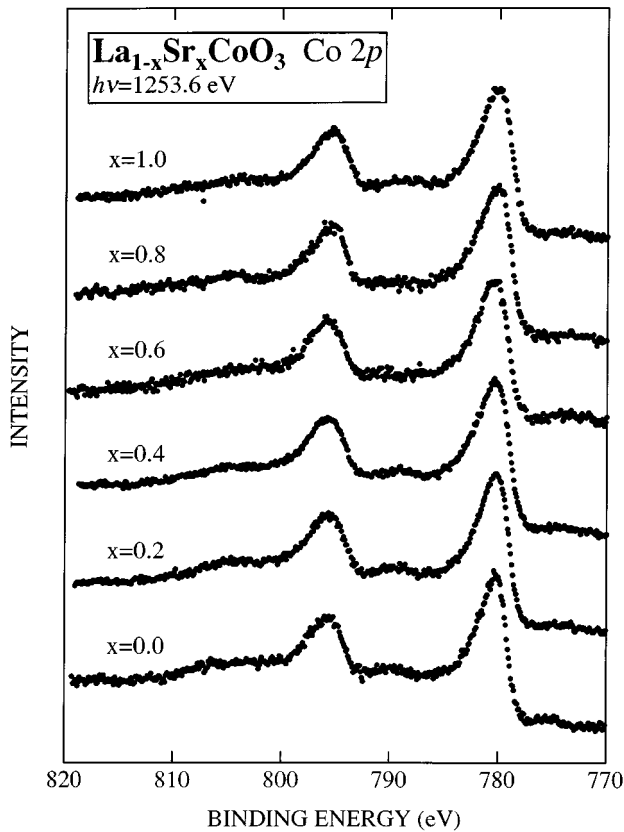


FIG. 2. Co 2*p* core-level XPS spectra of $\text{La}_{1-x}\text{Sr}_x\text{CoO}_3$. The intensity has been normalized to the $2p_{3/2}$ peak height. The weak peak at ~ 776 eV is attributed to O *KVV* Auger emission.

this region does not change so much with Sr doping and hence the above shifts may reflect the shift of E_F with hole doping. This is probably because the intensity of this region mainly comes from the oxygen nonbonding states (with some contributions from O $2p$ -Co $4sp$ and O $2p$ -La/Sr $5sd$ bonding states), which may show a minimal change in its shape with doping. The predominance of nonbonding oxygen states in this region can be seen in Fig. 5, which shows the intensity in this region is stronger in the He I spectra than in the He II spectra.¹⁹ Moreover, the He I spectra show exactly the same behavior with Sr doping as those of the He II spectra including the amount of the energy shifts, strongly supporting the above argument. On the other hand, with Sr doping, structure A continuously loses its spectral weight while structure D grows, thus increasing the bandwidth with hole doping. It is also noted that from Fig. 5 and spectra taken with higher photon energies reported previously,^{12,18} structure A becomes more intense with increasing photon energy. This means that structure A has a large Co $3d$ contribution,¹⁹ consistent with the resonant-photoemission spectra shown below.

The combined UPS and O $1s$ XAS spectra near E_F are displayed in Fig. 6. Here the O $1s$ XAS spectra have been normalized ~ 20 eV above the threshold, where the absorption intensity should be independent of x . By Sr doping, the intensity of structure A below E_F decreases and the peak of the O $1s$ XAS spectra grows, showing a transfer of spectral weight from the occupied to unoccupied states with hole doping.

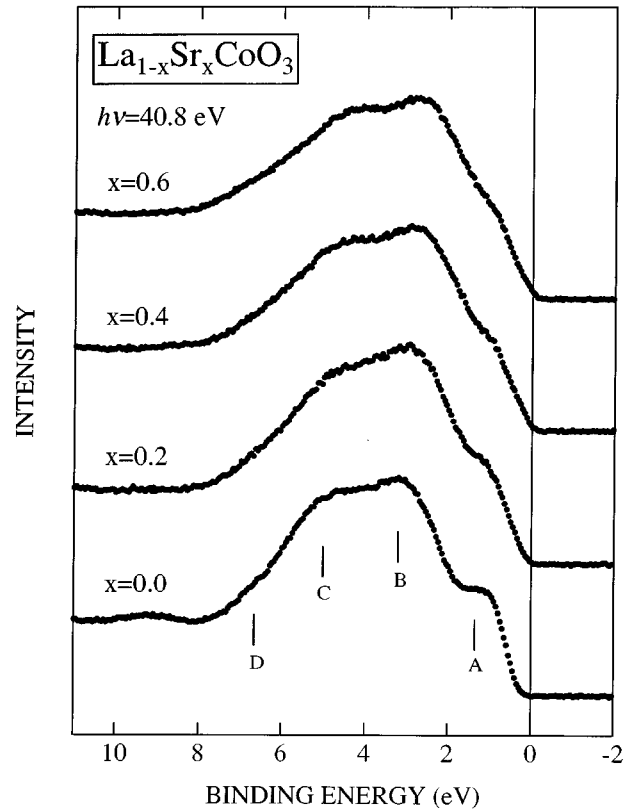


FIG. 3. He II UPS spectra of $\text{La}_{1-x}\text{Sr}_x\text{CoO}_3$. The intensity has been normalized to the total integrated intensity.

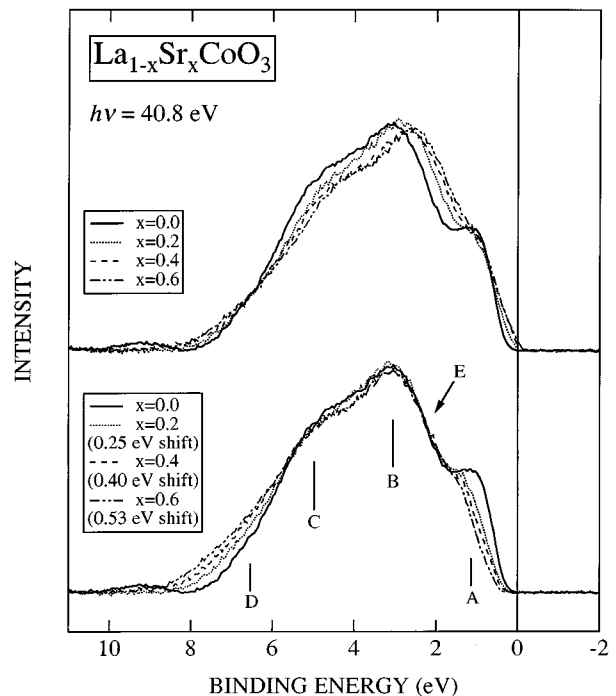


FIG. 4. He II UPS spectra of $\text{La}_{1-x}\text{Sr}_x\text{CoO}_3$. The background due to secondary electrons has been subtracted and the intensity has been normalized to the total integrated intensity. In the lower panel, the spectra for $x > 0$ have been shifted towards higher binding energy as indicated.

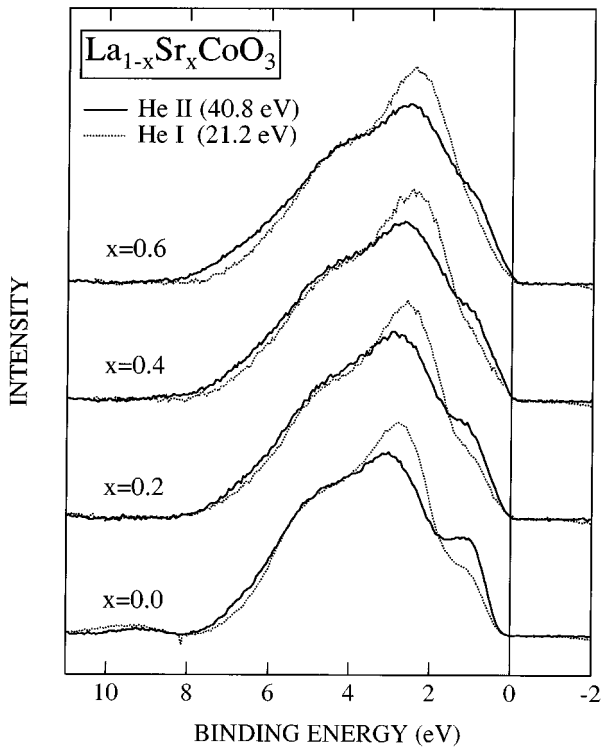


FIG. 5. Comparison of the He I (dotted lines) and He II (solid lines) spectra of $\text{La}_{1-x}\text{Sr}_x\text{CoO}_3$. The normalization is the same as in Fig. 4.

In order to extract Co $3d$ contribution from the valence-band spectra more directly, we have measured resonant-photoemission spectra near the Co $3p$ - $3d$ core-absorption threshold. The on- and off-resonance photon energies were determined from the total yield and constant-initial-state spectra. In Fig. 7, we show on- ($h\nu=63.5$ eV) and off- ($h\nu=60.0$ eV) resonance spectra of $\text{La}_{1-x}\text{Sr}_x\text{CoO}_3$. One can see that all the on-resonance spectra are enhanced over a wide energy range, with the strongest enhancement from ~ 8 eV to ~ 15 eV, which should be identified as a satellite due to O $2p$ -to-Mn $3d$ charge transfer. The on-off difference spectrum for LaCoO_3 shows an intense peak near E_F and a shoulder at ~ 6 eV (marked with two arrows) as well as the satellite centered at ~ 11 eV. It is worthwhile noting that apart from the enhancement of the satellite the experimental LaCoO_3 spectrum is in very good agreement with the calculated spectrum for the low-spin (1A_1) ground state using the configuration-interaction (CI) cluster model: the arrow-marked structures clearly correspond to the first two peaks in the calculated 1A_1 spectrum shown in the figure or the calculated spectrum for the $^1A_1 + ^3T_1$ mixed ground state.⁶ The overall feature does not change significantly with doping for $x=0.2$, but small changes can be observed for $x=0.4$: the first peak becomes broader and the shoulder at ~ 6 eV is weakened; the overall spectrum becomes broad and featureless. According to Itoh and Natori,²⁰ the intensity of signals from the nonmagnetic Co^{3+} ion in their NMR measurement decreased very rapidly with Sr doping, and no 1A_1 signal was detected in $x=0.4$. On the other hand, our recent calculations on LaCoO_3 have shown that the spectrum for the 5T_2 (high-spin) ground state is completely different from the

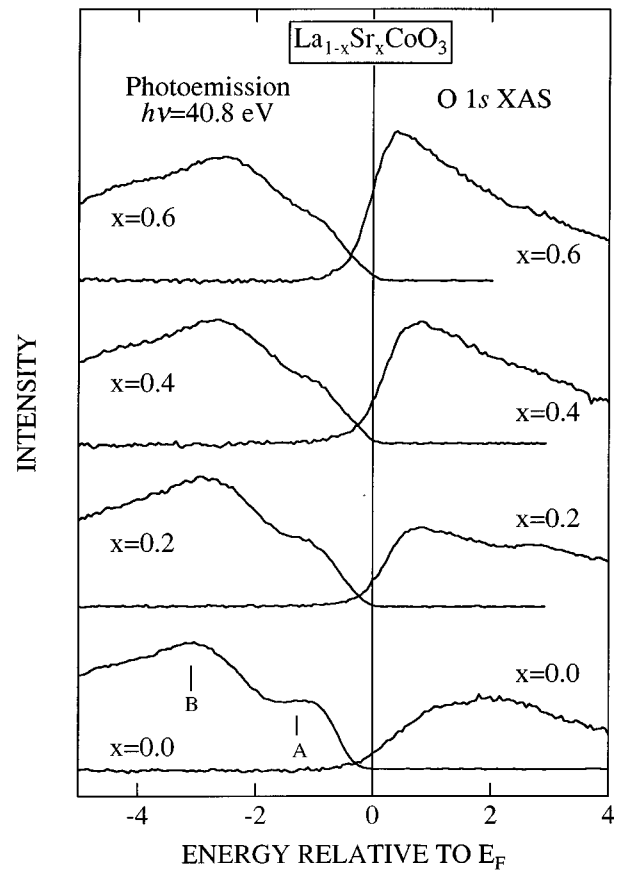


FIG. 6. UPS and O $1s$ XAS spectra of $\text{La}_{1-x}\text{Sr}_x\text{CoO}_3$ near E_F . Photon energies for the O $1s$ XAS spectra are references to the O $1s$ binding energies plus 1.0 eV.

1A_1 spectrum while the spectrum for the 3T_1 (intermediate-spin) ground state is much more similar to the 1A_1 spectrum.⁶ Hence the small change in the difference spectra suggests that the magnetic state is changing from 1A_1 to 3T_1 rather than from 1A_1 to 5T_2 .

In Fig. 8, the energy shifts of several core levels and a valence-band feature are plotted as functions of Sr concentration. The figure shows that the O $1s$ and La $3d$ core levels behave in the same way,²¹ and edge E also shows a similar shift up to $x=0.6$. Since the A-site ions in perovskite oxides ABO_3 are not involved in the chemical bonding nor in the metallic conductivity, the shifts of the La core levels would faithfully reflect the shift of E_F if the changes in the Madelung potential with x are negligibly small.²² Considering that the changes in the Madelung potential at the La cation site and the O anion site should be quite different, the same behavior of the La $3d$ and O $1s$ core-level shifts implies that the changes in the Madelung potential are effectively screened (within experimental errors) and that the La $3d$ and O $1s$ core-level shifts reflect the chemical-potential shift. The change in the Co $2p$ core-level position relative to the O $1s$ core level will thus represent the so-called chemical shift, which reflects the change of the valence of Co. On the other hand, the behavior of the core-level shifts for $x \geq 0.6$ is complicated. However, because the accurate determination of core-level shifts requires contamination/degradation-free surfaces as demonstrated in Ref. 22, we defer discussions

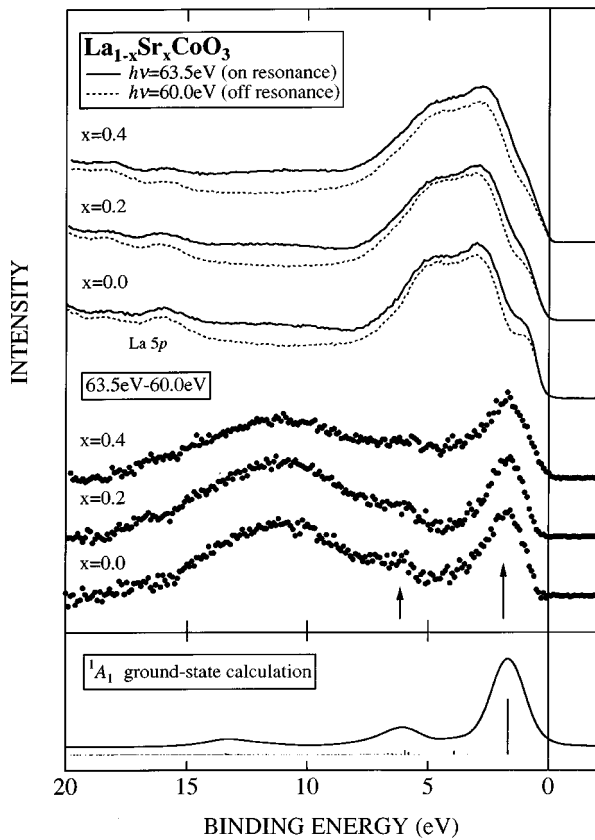


FIG. 7. Upper panel: Co $3p$ - $3d$ resonant-photoemission spectra of $\text{La}_{1-x}\text{Sr}_x\text{CoO}_3$. Lower panel: On-off difference spectra compared with a CI cluster-model calculation for the low-spin (1A_1) ground state (Ref. 6). For the experimental spectra, the background due to secondary electrons has been subtracted and the intensity has been normalized to the total integrated intensity.

about the chemical-potential shift for the $x \geq 0.6$ samples, the O $1s$ spectra of which (Fig. 1) indicate weak signals of contamination or degradation.

IV. DISCUSSIONS

With Sr doping, structure A at ~ 1 eV in the valence-band photoemission spectra loses its spectral weight and a tail towards E_F develops. This may be attributed to a change from the low-spin initial state to the high-spin or intermediate-spin initial state. The change of the on-off difference spectra with x (Fig. 7) is small, suggesting that the low-spin Co ions would not be converted to the high-spin states but more likely to the intermediate-spin ones. This scenario has been supported not only by our calculations on LaCoO_3 (Ref. 6) and the NMR study by Itoh and Natori²⁰ (see Chap. III), but also by another XAS study: recently, Potze *et al.* have proposed the possibility of the intermediate-spin ground state ($t_{2g}^4 e_g^1$, $S = 3/2$) in SrCoO_3 from Co $2p$ XAS.¹³ According to these authors, the dominant configuration in the ground state of SrCoO_3 is not d^5 but $d^6\bar{L}$ due to the negative charge-transfer energy. This is consistent not only with our results but also with the small saturation magnetization of $\text{La}_{1-x}\text{Sr}_x\text{CoO}_3$.^{7,9}

Electrons in the metallic phase of $\text{La}_{1-x}\text{Sr}_x\text{CoO}_3$ are

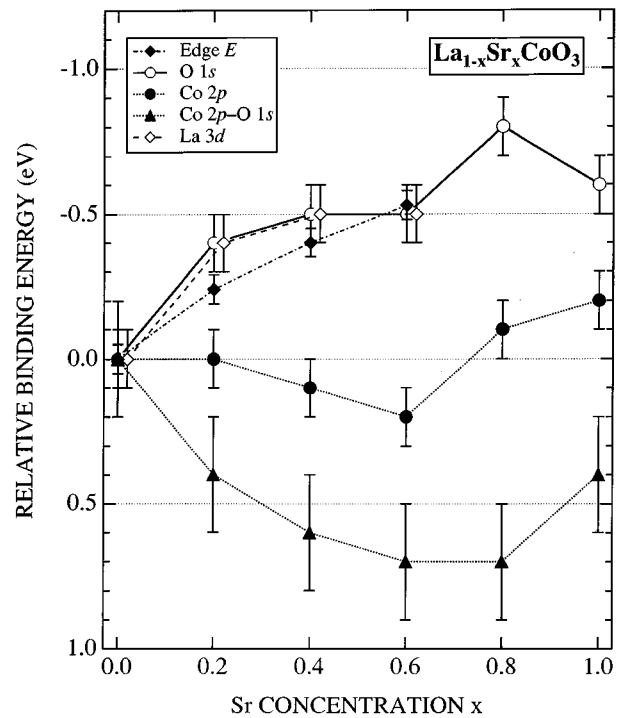


FIG. 8. Energy shifts of the core and valence levels in $\text{La}_{1-x}\text{Sr}_x\text{CoO}_3$ as functions of Sr concentration x . The Co $2p$ core-level energy position relative to the O $1s$ core level is also shown.

considered to be much more itinerant than those of $\text{La}_{1-x}\text{Sr}_x\text{MnO}_3$ because of the stronger hybridization in the former system. This is also supported by the fact that $\text{La}_{1-x}\text{Sr}_x\text{CoO}_3$ has a much higher Fermi-edge intensity than $\text{La}_{1-x}\text{Sr}_x\text{MnO}_3$ in the photoemission spectra.^{16,17} In the band picture, the strong p - d hybridization would reduce the exchange splitting of the t_{2g} bands, resulting in the small saturation magnetization in the heavily doped metallic phase.

Recently, Yamaguchi *et al.*²³ have found that a hole doped into LaCoO_3 induces a large magnetic moment and concluded that the doped hole creates a spin polaron which is spread over ~ 5 – 8 sites. This is consistent with the rapid decrease in the intensity of the 1A_1 signal in the NMR measurement.²⁰ Thus, the spin-glass behavior in the lightly doped phase¹¹ can be attributed to the competition between the double exchange interaction and the superexchange interaction between the spins of e_g electrons. Also we may speculate that the cluster-glass behavior in the heavily doped phase¹¹ might be accounted for by the increase in the ferromagnetic correlation due to the double exchange interaction. The spin-glass behavior or the cluster-glass behavior have not been observed in $\text{La}_{1-x}\text{Sr}_x\text{MnO}_3$, which can be understood as a result of the weaker superexchange interaction in the latter system arising from the fact that each e_g electron has a smaller probability to find another e_g electron at adjacent sites due to the smaller number ($1-x$ per site) of e_g electrons than that (~ 1 per site in the intermediate-spin state) in $\text{La}_{1-x}\text{Sr}_x\text{CoO}_3$.

From the viewpoint of the local electronic structure, the weaker MR in $\text{La}_{1-x}\text{Sr}_x\text{CoO}_3$ than in $\text{La}_{1-x}\text{Sr}_x\text{MnO}_3$ may be explained by the stronger hybridization caused by the smaller charge-transfer energy than the Mn system. This

makes the ground state of LaCoO_3 low-spin and leads to the intermediate-spin state in the ferromagnetic phase and hence the small saturation magnetization. Another important reason for the weaker MR in $\text{La}_{1-x}\text{Sr}_x\text{CoO}_3$ is the absence of Jahn-Teller effect in contrast to $\text{La}_{1-x}\text{Sr}_x\text{MnO}_3$: in the latter system, it has been pointed out that the Jahn-Teller distortion plays an important role in the ‘‘colossal’’ magnetoresistance.²⁴ On the other hand, $\text{La}_{1-x}\text{Sr}_x\text{FeO}_3$, located between the Mn and the Co systems, is not a double exchange system because it remains insulating in most of the doping range due to the multiplet effect, i.e., the stabilization of the d^5 configuration due to Hund’s rule coupling.²⁵

V. CONCLUSIONS

We have studied the electronic structure of $\text{La}_{1-x}\text{Sr}_x\text{CoO}_3$ by photoemission and x-ray absorption spectroscopy. The Co $2p$ core-level and the valence-band spectra display satellite structures, indicating correlation effects. The doping dependence shows the evolution of spectral line shape from the low-spin semiconductor to the metal, which is not rigid-band like: with Sr doping, the structure at the lowest binding energy loses its intensity and becomes

broad. The lost spectral weight is transferred to the unoccupied states, as observed in the O $1s$ XAS spectra. At the same time, spectral weight near E_F increases. The entire valence band is shifted towards E_F with doping, representing a downward chemical-potential shift with hole doping. Combined with the CI cluster-model calculations on LaCoO_3 , the small changes in the resonant-photoemission spectra suggest that the intermediate-spin state may be realized in the ferromagnetic phase.

ACKNOWLEDGMENTS

We would like to thank Y. Tezuka and S. Shin of SRL, M. F. Lopez, O. Strebels, M. Domke, and G. Kaindl of Freie Universität der Berlin for technical support. We would also like to thank T. Katsufuji, Y. Okimoto, and D. D. Sarma for valuable discussions. The present work is supported by the Japan Society for the Promotion of Science for Japanese Junior Scientists, a Grant-in-Aid for Scientific Research from the Ministry of Education, Science and Culture and the New Energy and Industrial Technology Development Organization (NEDO).

*Present address: Department of Physics, University of Colorado, Boulder, Colorado 80309-0390.

¹K. Chahara, T. Ohno, M. Kasai, and Y. Kozono, *Appl. Phys. Lett.* **63**, 1990 (1993); R. von Helmolt, J. Wecker, B. Holzappel, L. Schultz, and K. Samwer, *Phys. Rev. Lett.* **71**, 2331 (1993); Y. Tokura, A. Urushibara, Y. Moritomo, T. Arima, A. Asamitsu, G. Kido, and N. Furukawa, *J. Phys. Soc. Jpn.* **63**, 3931 (1994).

²C. Zener, *Phys. Rev.* **82**, 403 (1951); P. W. Anderson and H. Hasegawa, *ibid.* **100**, 675 (1955); P.-G. deGennes, *ibid.* **118**, 141 (1960).

³S. Yamaguchi, H. Taniguchi, H. Takagi, T. Arima, and Y. Tokura, *J. Phys. Soc. Jpn.* **64**, 1885 (1995).

⁴G. Briceno, X.-D. Xiang, H. Chang, X. Sun, and P. G. Schultz, *Science* **270**, 273 (1995).

⁵M. A. Korotin, S. Yu. Ezhov, I. V. Solovyev, V. I. Anisimov, D. I. Khomskii, and G. A. Sawatzky, *Phys. Rev. B* **54**, 5309 (1996).

⁶T. Saitoh, T. Mizokawa, A. Fujimori, M. Abbate, Y. Takeda, and M. Takano, *Phys. Rev. B* **55**, 4257 (1997).

⁷G. H. Jonker and J. H. van Santen, *Physica (Amsterdam)* **19**, 120 (1953).

⁸P. M. Raccah and J. B. Goodenough, *J. Appl. Phys.* **39**, 1209 (1968).

⁹H. Taguchi, M. Shimada, and M. Koizumi, *Mater. Res. Bull.* **13**, 1225 (1978); *J. Solid State Chem.* **33**, 169 (1980); **29**, 221 (1979).

¹⁰G. H. Jonker and J. H. van Santen, *Physica (Amsterdam)* **16**, 337 (1950); A. Urushibara, Y. Moritomo, T. Arima, A. Asamitsu, G. Kido, and Y. Tokura, *Phys. Rev. B* **51**, 14 103 (1995).

¹¹M. Itoh, I. Natori, S. Kubota, and K. Motoya, *J. Phys. Soc. Jpn.* **63**, 1486 (1994).

¹²A. Chainani, M. Mathew, and D. D. Sarma, *Phys. Rev. B* **46**, 9976 (1992).

¹³R. H. Potze, G. A. Sawatzky, and M. Abbate, *Phys. Rev. B* **51**, 11 501 (1995).

¹⁴Z. L. Wang and Jiming Zhang, *Phys. Rev. B* **54**, 1153 (1996).

¹⁵B. W. Veal and D. J. Lam, *J. Appl. Phys.* **49**, 1461 (1978); D. J. Lam, B. W. Veal, and D. E. Ellis, *Phys. Rev. B* **22**, 5730 (1980).

¹⁶T. Saitoh, A. E. Bocquet, T. Mizokawa, H. Namatame, A. Fujimori, M. Abbate, Y. Takeda, and M. Takano, *Phys. Rev. B* **51**, 13 942 (1995).

¹⁷D. D. Sarma, N. Shanthi, S. R. Krishnakumar, T. Saitoh, T. Mizokawa, A. Sekiyama, K. Kobayashi, A. Fujimori, E. Weschke, R. Meier, G. Kaindl, Y. Takeda, and M. Takano, *Phys. Rev. B* **53**, 6873 (1996).

¹⁸R. P. Vasquez, *Phys. Rev. B* **54**, 14 938 (1996).

¹⁹J. J. Yeh and I. Lindau, *At. Data Nucl. Data Tables* **32**, 1 (1985).

²⁰M. Itoh and I. Natori, *J. Phys. Soc. Jpn.* **64**, 970 (1995).

²¹The same energy shifts on $\text{La}_{1-x}\text{Ca}_x\text{CoO}_3$ have been reported in Ref. 18.

²²A. Ino, T. Mizokawa, A. Fujimori, K. Tamasaku, H. Eisaki, S. Uchida, T. Kimura, T. Sasagawa, and K. Kishio (unpublished).

²³S. Yamaguchi, Y. Okimoto, H. Taniguchi, and Y. Tokura, *Phys. Rev. B* **53**, 2926 (1996).

²⁴For example, A. J. Millis, P. B. Littlewood, and B. I. Shraiman, *Phys. Rev. Lett.* **74**, 5144 (1995).

²⁵T. Saitoh, A. E. Bocquet, T. Mizokawa, and A. Fujimori, *Phys. Rev. B* **52**, 7934 (1995).